LA-UR -91-117

Los Alamos National Laboratory is operated by the University of California for the United States Department of Energy under contract W-7405-ENG-36

LA-UR--91-117

DE91 007387

TITLE EXTENSION OF THE FULLY COUPLED MONTE CARLO/SN RESPONSE MATRIX METHOD TO PROBLEMS INCLUDING UPSCATTER AND FISSION

AUTHOR(S) Randal S. Baker
Raymond E. Alcouffe
William F. Filippone

SUBMITTED TO For publication in the proceedings of the ANS Pittsburgh 1991 International Topical Meeting on "Advances in Mathematics, Computations, and Reactor Physics," to be held April 28-May 1, 1991, in Greentree Marriott, Pittsburgh, PA

DISCLAIMER

Los Alamos Los Alamos National Laboratory
Los Alamos, New Mexico 87545

EXTENSION OF THE FULLY COUPLED MONTE CARLO/S_N RESPONSE MATRIX METHOD TO PROBLEMS INCLUDING UPSCATTER AND FISSION

R. S. Baker
University of Arizona, Department of Nuclear & Energy Engineering
Tucson, Arizona 85721

R. E. Alcouffe
Los Alamos National Laboratory
Applied Theoretical Physics Division, Los Alamos, New Mexico 87545

W. L. Filippone
University of Arizona, Department of Nuclear & Energy Engineering
Tucson, Arizona 85721

ABSTRACT

The neutron transport equation is solved by a hybrid method that iteratively couples regions where deterministic (S_N) and stochastic (Monte Carlo) methods are applied. Unlike previous hybrid methods, the Monte Carlo and S_N regions are fully coupled in the sense that no assumption is made about geometrical separation or decoupling. The fully coupled Monte Carlo/S_N technique consists of defining spatial and/or energy regions of a problem in which either a Monte Carlo calculation or an S_N calculation is to be performed. The Monte Carlo and S_N regions are then connected through the common angular boundary fluxes, which are determined iteratively using the response matrix technique, and group sources. The hybrid method provides a new method of solving problems involving both optically thick and optically thin regions that neither Monte Carlo nor S_N is well suited for by itself.

The fully coupled Monte Carlo/S_N method has been implemented in the S_N code TWODANT by adding special-purpose Monte Carlo subroutines to calculate the response matrices and group sources, and linkage subroutines to carry out the interface flux iterations. The common angular boundary fluxes are included in the S_N code as interior boundary sources, leaving the logic for the solution of the transport flux unchanged, while, with minor modifications, the diffusion synthetic accelerator remains effective in accelerating the S_N calculations. The Monte Carlo routines have been succesfully vectorized, with approximately a factor of five increase in speed over the non-vectorized version.

The hybrid method is capable of solving forward, inhomogeneous source problems in $X - Y$ and $R - Z$ geometries. This capability now includes mulitigroup problems involving upscatter and fission in non-highly multiplying ($k_{eff} \leq .8$) systems. The hybrid method has been applied to several challenging test problems with good results.

INTRODUCTION AND BACKGROUND

In the fully coupled Monte Carlo/S_N response matrix method, spatial and/or energy regions of a problem are defined in which either a Monte Carlo or an S_N calculation is performed. The regions are then connected through the common boundary fluxes, for spatial interfaces, and group sources, for energy interfaces. The fully coupled Monte Carlo/S_N technique differs from previous coupling methods[1] in that no assumptions are made about geometric separation or decoupling. Instead, the common boundary fluxes at a Monte Carlo/S_N spatial interface are determined through an iterative process which uses a precalculated response matrix for the Monte Carlo region, and standard S_N techniques in the S_N region. Thus, the fully coupled technique is ideally suited for problems involving both optically thick and optically thin regions which are tightly coupled, with the Monte Carlo technique being used in the optically thin region, and the S_N technique in the optically thick.

The practicality of the fully coupled Monte Carlo/S_N technique was first demonstrated for simple, one-group neutron transport problems in $X-Y$ geometry with an inhomogeneous source in the Monte Carlo region.[2] The hybrid method was implemented in the S_N code TWODANT[3] by adding special-purpose Monte Carlo and linkage subroutines. Interior boundary sources were included in TWODANT to provide a link to the Monte Carlo region, leaving the logic for the transport sweeps and Diffusion Synthetic Acceleration (DSA) accelerator[4] essentially unchanged, although the efficiency of the DSA accelerator was reduced by discontinuities in the tranport operator when sweeping across an Monte Carlo/S_N interface. Reference 2 determined that the preferred location for the interface between the Monte Carlo and S_N regions was approximately one mean free path into the the optically thick region. Although this reduces the efficiency of the Monte Carlo calculation, since it increases the number of scattering events, the inclusion of a boundary layer places the Monte Carlo/S_N interface in a region where the angular flux is not as highly anisotropic. Thus, the angular flux can be described by a lower-order S_N quadrature set, reducing the size of the response matrix. In reference 5, the hybrid technique was succesfully extended to more general problems, including $R-Z$ geometries and multigroup problems involving downscatter only. However, the test problems were limited to just three groups with fictitous cross sections such that the size of the boundary layer did not vary with energy group.

To be able to solve more realistic problems, we have now extended the fully coupled Monte Carlo/S_N technique to include upscatter, fission, and variable boundary layers. Furthermore, the Monte Carlo algorithms have been vectorized to reduce computation time, and the full effectiveness of the DSA accelerator has been restored.

THEORY AND IMPLEMENTATION

Let Ψ_g^{in} and Ψ_g^{out} be defined as the angular boundary fluxes entering and leaving the group g Monte Carlo region, respectively, where each element corresponds to a unique combination (state) of spatial cell and quadrature direction. For the pure downscatter case, the angular boundary fluxes are determined by the iteration procedure

$$\Psi_g^{out(r+1)} = \mathbf{R}_{gg}\,\Psi_g^{in(r)} + \mathbf{Q}_g^{out}, \qquad g = 1,\ldots,G, \tag{1}$$

with

$$\mathbf{Q}_g^{out} = \sum_{g'<g} \mathbf{R}_{gg'}\,\Psi_{g'}^{in(\infty)} + \mathbf{S}_g^{out}, \tag{2}$$

where the jj'th element of the response submatrix $\mathbf{R}_{gg'}$ represents the angular flux leaving the group g Monte Carlo region in S_N state j due to a unit incident angular flux in S_N state j' of group g', and $\mathbf{S}_g^{out}$ is the exiting flux from the Monte Carlo region under vacuum boundary conditions (i.e., the outgoing angular boundary source due to the fixed source inside the Monte Carlo region). Note that $\mathbf{R}_{gg}$ and $\mathbf{S}_g^{out}$ are precalculated by Monte Carlo techniques, while $\Psi_g^{in(r)}$ is obtained by using an S_N solver with the prescribed boundary flux $\Psi_g^{out(r)}$, with one S_N calculation per iteration step r. Instead of calculating the response matrices $\mathbf{R}_{gg'}$, the downscatter contribution to $\mathbf{Q}_g^{out}$ is determined by sampling the $\Psi_g^{in(\infty)}$ directly using Monte Carlo, where $\Psi_g^{in(\infty)}$ represents the converged incoming angular boundary flux. With this formulation, the direct calculation of $\mathbf{R}$ is replaced by the calculation of G submatrices $\mathbf{R}_{gg}$, and G samplings of the incoming boundary fluxes $\Psi_g^{in(\infty)}$. Since only one submatrix $\mathbf{R}_{gg}$ is required at any given time, the remainder can be stored on disk, reducing memory requirements by a factor of G^2.

To extend the hybrid method to problems including upscatter and fission, we include an outer iteration p, and replace Equations (1) and (2) with

$$\Psi_g^{out(p+1,r+1)} = \tilde{\mathbf{R}}_{gg}\,\Psi_g^{in(p+1,r)} + \mathbf{Q}_g^{out(p)}, \qquad g = 1,\ldots,G, \tag{3}$$

and

$$\mathbf{Q}_g^{out(p)} = \sum_{g'<g} \mathbf{R}_{gg'}\,\Psi_{g'}^{in(p+1,\infty)} + \sum_{g'>g} \mathbf{R}_{gg'}\,\Psi_{g'}^{in(p,\infty)} + (\mathbf{R}_{gg} - \tilde{\mathbf{R}}_{gg})\,\Psi_g^{in(p,\infty)} + \mathbf{S}_g^{out}. \tag{4}$$

When sampling the response submatrix $\mathbf{R}_{gg}$, we increase the efficiency of the calculation by removing the possibility of upscatter or downscatter, so that we actually determine a biased submatrix which we denote by $\tilde{\mathbf{R}}_{gg}$. We remove the bias when sampling the incoming boundary flux $\Psi_g^{in(p+1,\infty)}$ by scoring in $\mathbf{Q}_g^{out(p+1)}$ particles which scatter out of group g at some point, but latter scatter back in and cross the group g Monte Carlo/S_N interface.

With this implementation, we possibly perform G additional Monte Carlo calculations for each outer iteration p, since we must sample the $\Psi_g^{in(p+1,\infty)}$ for each group g in which a Monte Carlo/S_N spatial interface exists. The expense of this would rapidly become prohibitive for slowly converging problems in p. More importantly, the resulting statistical variations in the source term would preclude any possibility of meeting the S_N pointwise convergence criteria, which are typically on the order of 10^{-4}. Thus, we replace the sampling of $\Psi_g^{in(p+1,\infty)}$ with the sampling of $\delta\Psi_g^{in(p+1,\infty)}$, where

$$\delta\Psi_g^{in(p+1,\infty)} = \Psi_g^{in(p+1,\infty)} - \Psi_g^{in(p,\infty)}. \tag{5}$$

Since we are now sampling only the difference between the incoming boundary fluxes, convergence of the S_N region source term is not impeded by statistical fluctations in the Monte Carlo region, and as the magnitude of $\delta\Psi_g^{in(p+1,\infty)}$ decreases, we reduce the number of histories used to sample it. With this formulation, Equation (4) becomes

$$\begin{aligned}\mathbf{Q}_g^{out(p)} = &\sum_{p'=1}^{p}\sum_{g'<g} \mathbf{R}_{gg'}\,\delta\Psi_{g'}^{in(p'+1,\infty)} + \sum_{p'=1}^{p-1}\sum_{g'>g} \mathbf{R}_{gg'}\,\delta\Psi_{g'}^{in(p'+1,\infty)} \\ &+ \sum_{p'=1}^{p-1} (\mathbf{R}_{gg} - \tilde{\mathbf{R}}_{gg})\,\delta\Psi_g^{in(p'+1,\infty)} + \mathbf{S}_g^{out}.\end{aligned} \tag{6}$$

If the S_N operator were strictly linear, we would expect the $\delta\Psi_g^{in(p+1,\infty)}$ to be non-negative. Due to the use of negative flux fix-up in the S_N, however, this is not the case. While it is generally advantageous to avoid introducing particles with negative weights in Monte Carlo calculations, we assume that, in this case, the magnitude of any negative residuals will be small enough so that it will not adversely affect the hybrid results. Thus, when an element of $\delta\Psi_g^{in(p+1,\infty)}$ is negative, we assign negative weights to the particles used to sample that state.

As previously mentioned, with real cross sections the size of the optically thick boundary layer included in the Monte Carlo region will be group dependent. Variable boundary layer thicknesses have now been implemented in the hybrid method. For Monte Carlo calculations, when a particle scatters out of group g we check to see if its new group value places it in an S_N region. If so, we score it as a cell-centered angular flux. At the conclusion of the Monte Carlo calculation, we integrate the resulting angular fluxes to get moments, which are then placed in the appropriate S_N array.

Cross sections for the Monte Carlo region are obtained from the discrete ordinates multigroup cross section set. Angular scattering is represented in terms of equiprobable bins[6] defined so as to approximately conserve the moments $\int_{-1}^{+1} d\mu_0^L \sigma_L(\mu_0)$ of the truncated angular scattering cross section $\sigma_L(\mu_0)$. While currently restricted to isotropic scattering ($L = 0$), we plan to extend the hybrid method to include anisotropic scattering by incorporating a code which calculates equiprobable bins for $L > 0$.

Sources located in the group g Monte Carlo region as a result of S_N calculations are sampled prior to the iteration procedure of Equation (4). The cell-centered angular fluxes are reconstructed from the S_N moments and sampled using Monte Carlo. Particles which then cross a Monte Carlo/S_N spatial interface in group g' are stored in $\mathbf{Q}_{g'}^{out(p)}$, while those which scatter into an S_N region are scored as above. As in the case for the incoming boundary fluxes, we actually sample the residual source $\delta\mathbf{Q}_{g'}^{out(p)}$, and allow the possibility of negative residual sources.

The special-purpose Monte Carlo subroutines implemented with TWODANT are basically analog routines, with no variance reduction techniques used other than implicit capture and stratified sampling. To increase the efficiency of the Monte Carlo calculations, we have recently vectorized the Monte Carlo subroutines. The Monte Carlo routines are vectorized through the formation of event-based stacks,[7] where each stack ideally consists of a group of 64 particles undergoing an identical event, such as a collision. Cray Assembly Language (CAL) routines are used to encode particle destination tag words, and to move particles between stacks. Vectorization resulted in a factor of four to five increase in speed of the vectorized Monte Carlo routines over the non-vectorized Monte Carlo routines.

The Monte Carlo region is linked to the S_N region in TWODANT through the inclusion of interior boundary sources, so that sweeping algorithms are unaffected. However, the inclusion of interior boundary sources does affect the operation of the DSA accelerator, either reducing its effectiveness, or eliminating it entirely for some problems. This loss of effectiveness is essentially due to the introduction of a discontinuity in the transport equation. Consider an S_N sweep along a quadrature direction which begins in an S_N region, passes through the Monte Carlo region, and back out into an S_N region. As the transport sweep enters into the Monte Carlo region, we continue to determine the cell fluxes as normal, even though the S_N values are subsequently replaced by Monte Carlo determined values. However, when the sweep crosses the Monte Carlo/S_N interface back into an S_N region, we replace the S_N calculated values for the cell-edge fluxes with the

interior boundary souce determined from Equation (3). It is this discontinuity in the transport operator which interferes with the operation of the DSA accelerator.

To remove this discontinuity from the DSA equations, we set the within-group scattering sources inside the Monte Carlo region to zero and replace the interior boundary sources with an inhomogeneous source located inside the Monte Carlo region which gives approximately the same boundary source. This construction has proven to be as succesful in accelerating the inner iterations as the standard DSA method, i.e., the number of inner iterations required for an S_N calculation in the hybrid method is less than or equal to the number of inner iterations required by the standard S_N method.

RESULTS

We have applied the hybrid Monte Carlo/S_N technique to a sample problem in $X - Y$ geometry consisting of two uranium oxide plates with a density of 10 gm/cm^3, 100% enriched in U^{235}, separated by an aluminum plate with a density of 3 gm/cm^3 (Figure 1). Each uranium plate has a width of 5 cm, while the width of the aluminum plate is 3 cm. The overall dimensions of the block are 10 cm by 13 cm. The aluminum plate, plus a boundary layer of uranium of width 1 mean free path, is designated as the Monte Carlo region.

We use a sixteen-group Hansen-Roach cross section set, with an isotropic surface flux in group 1 incident on the left-hand edge of the block between $y = 6$ and $y = 7$ cm, that is, incident on the center of the left-hand edge of the aluminum plate. With a 1 mean free path (mfp) boundary layer, the Monte Carlo region comprises the entire spatial geometry for the first two energy groups, with spatial Monte Carlo/S_N interfaces in groups 3 through 7 (Figure 2). We designate groups 8 through 16 as S_N only groups.

Examining the total reaction rates at the right-hand side of the block for group 1 (Figure 3), we see that while the hybrid Monte Carlo/S_8 results agree closely with the Monte Carlo benchmark, a standard S_8 calculation exhibits severe ray effects. In order to obtain results wihin 5% of the hybrid and Monte Carlo results, an S_{30} calculation with a refined spatial mesh is required. By group 6 (Figure 4), the S_N no longer suffers from ray effects, and all calculations are in good agreement for both the left and right-hand edge reaction rates, although we see some statistical variations starting to affect both the Monte Carlo and hybrid results. We note, however, that the hybrid method was able to calculate accurate integral leakage results for all 16 groups (Figure 5), while the (analog) Monte Carlo calculation was not, returning zero values for the lower energy groups. The hybrid technique used 145 CPU seconds, the Monte Carlo calculation 155 CPU seconds, and the S_{30} calculation 458 CPU seconds. The hybrid calculation required 7 outer iterations for convergence, while the S_{30} calculation needed 6. Approximately 90% of the CPU time in the hybrid calculation was spent in Monte Carlo subroutines.

We have also applied the hybrid method to a sample problem in $R - Z$ geometry consisting of a beam tube with a pure U^{235} target. The target has a 1 cm radius and is 2 cm thick, while the tube walls consist of 1 cm thick aluminum. The entire apparatus is surrounded by 10 cm of polyethylene ($C_5\,H_8\,O_2$) shielding (Figure 6). The beam source is composed of 14 MeV neutrons originating at a distance of 10 cm from the target. We use a 30-group MENDF5 cross section set with isotropic scattering. The interior of the beam tube and the U^{235} target are designated as the Monte Carlo region, and we specify a 1 mfp boundary layer, resulting in the spatial Monte

Carlo/S_N interface for the source energy group (group 2) shown at Figure 6. We use the S_N method in all other groups.

Because of the beam source, even a standard S_{80} calculation provides poor results. Instead, we compare a hybrid Monte Carlo/S_8 calculation with a multigroup (MG) MCNP[8] calculation. (We use the multigroup version of MCNP since it allows us to use the same cross section set used in the hybrid calculation.) Table 1 compares the energy-integrated right, bottom, and top leakages calculated by the two methods, as well as the scalar flux in the U^{235} target. The associated relative errors are shown for the MCNP (MG) values, as well as the difference (in standard deviations σ) between the hybrid and MCNP results. From Table 1, we see that the top and right leakages, as well as the scalar flux in the uranium target, are in good agreement (within two standard deviations). The bottom leakage, which is somewhat more sensitive to the S_N quadrature order than the other values, is still within three standard deviations of the MCNP result. While we do not directly compute a variance for the hybrid results, we note that the error in the fluxes in the Monte Carlo region due to the sampling of the source was less than 3%, while the $L2$ norm of the estimated error in the boundary fluxes was approximately 1%. For this problem, approximately 80% of the CPU time for the hybrid calculation was spent in Monte Carlo subroutines.

Figure 7 shows the top leakage as a function of energy group, while Figure 8 shows the group fluxes in the uranium target. From Figures 7 and 8, we see that the hybrid results are in good agreement with the MCNP (MG) results throughout the entire energy spectrum, and appear to have less variance in the lower energy groups. (Note that no energy splitting was used in the MCNP calculation).

By applying the hybrid method to the beam problem, and using the Monte Carlo method in selected spatial and energy regions, we are able to obtain results with an S_8 quadrature order that we are unable to achieve with even a standard S_{80} calculation that required over ten times the amount of CPU time as the hybrid method. And by using the S_N method in regions where the angular and spatial dependence of the problem are easily described by lower-order quadrature sets and reasonably sized mesh cells, we are able to achieve results comparable to an MCNP calculation at only a fifth the cost. Furthermore, the hybrid method provides detailed spatial and energy information, while attempting to provide the same level of information with MCNP would require the use of many more histories, even with additional variance reduction techniques.

DISCUSSION

The hypothesis of the hybrid Monte Carlo/S_N method is that, by coupling the two methods together in the same problem, we can solve certain types of problems more efficiently than either the Monte Carlo method or the S_N method can by themselves. The results shown above clearly demonstrate that this hypothesis holds even for semi-complex problems with fission and real cross section sets. The fully coupled Monte Carlo/S_N method appears to show real promise as an alternative solution method for problems involving both optically thin and optically thick regions, or problems with geometrically complicated and geometrically simple regions. The hybrid method also allows selected energy groups to be solved by the Monte Carlo method, while the remainder are solved by S_N methods, and can treat general sources, including those that contain singularities from an S_N point of view, naturally by using Monte Carlo.

Before we can apply the hybrid method to more general problems, however, we need to add additional capabilities. Of course, we need to add the capability to process anisotropic scattering

cross sections, and, if we wish to apply the method to highly multiplying mediums, some means of accelerating the outer iterations. We also need to use more sophisticated Monte Carlo techniques that allow geometries other than $X - Y$ and $R - Z$ in the Monte Carlo region, along with enhanced variance reduction techniques. More problematical, it would be highly desirable to provide more rigorous error estimates than are currently available in the hybrid method. Aside from the last item, however, it seems clear that there are no significant remaining obstacles towards the development of a generally useful hybrid Monte Carlo/S_N code. We believe that further development of such a code is warranted, and that it will furnish an attractive alternative to existing solution methods for certain types of problems.

REFERENCES

[1] M. B. Emmett, C. W. Burgart, and T. J. Hoffman, "Domino, A General Purpose Code for Coupling Discrete Ordinates and Monte Carlo Radiation Transport Calculations", ORNL-4853 (1973).

[2] W. L. Filippone and R. E. Alcouffe, "The S_N/Monte Carlo Response Matrix Hybrid Method", *Nucl. Sci. Eng.*, **100**, 209 (1988).

[3] R. E. Alcouffe, F. W. Brinkley, D. R. Marr, and R. D. O'Dell, "User's Guide for TWODANT: A Code Package for Two-Dimensional, Diffusion Accelerated, Neutral-Particle Transport", LANL LA-10049-M, Rev. 1 (1984).

[4] R. E. Alcouffe, "Diffusion Synthetic Acceleration Methods for the Diamond-Differenced Discrete-Ordinates Equations", *Nucl. Sci. Eng.*, **64**, 322 (1977).

[5] R. S. Baker, W. L. Filippone, and R. E. Alcouffe, "The Multigroup and Cylindrical Geometry Formulation of the Fully Coupled Monte Carlo/S_N Method", *Nucl. Sci. Eng.*, **105**, 184 (1990).

[6] L. L. Carter and C. A. Forrest, "Transfer Matrix Treatments for Multigroup Monte Carlo Calculations - the Elimination of Ray Effects", *Nucl. Sci. Eng.*, **59**, 27 (1976).

[7] F. W. Bobrowicz, K. J. Fisher, and R. G. Brickner, "Vectorized Monte Carlo Neutron Transport", LANL LA-UR-84-1269 (1984).

[8] Los Alamos Radiation Transport Group, "MCNP - A General Purpose Monte Carlo Code for Neutron and Photon Transport", LANL LA-7396-M, Rev. 2 (1986).

Table 1. Hybrid Method/MCNP Comparisons, Beam Problem

	MC/S_8	MCNP (MG)	Difference
Right Leakage (p/sec)	5.58e-1	5.66e-1 (.0084)	1.7σ
Top Leakage (p/sec)	3.54e-1	3.52e-1 (.0088)	0.6σ
Bottom Leakage (p/sec)	1.74e-1	1.67e-1 (.0158)	2.7σ
U^{235} Flux (p/cm^2-sec)	4.59e-1	4.55e-1 (.0048)	1.8σ
CPU Time (sec)	103.6	595.8	-

p - Particles per Source Particle

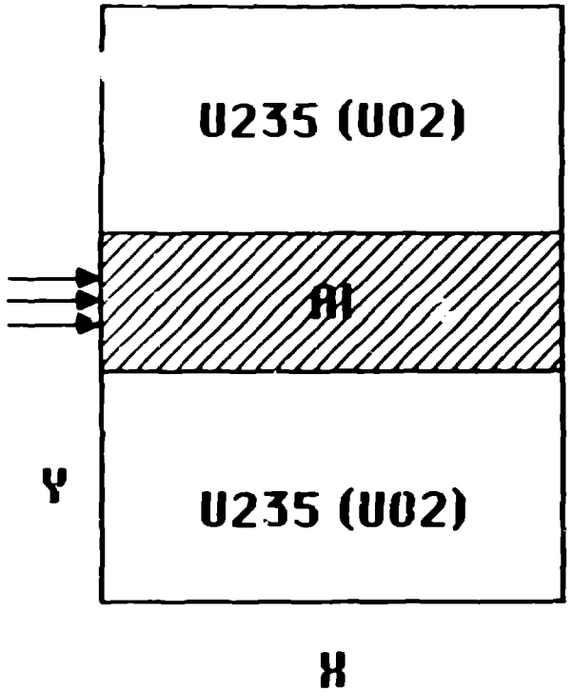

Fig. 1. A1/U235 problem geometry.

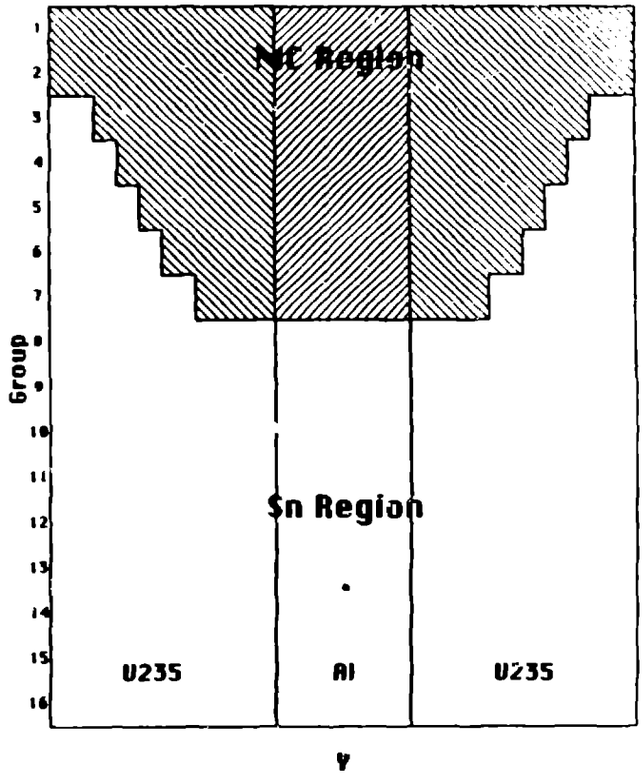

Fig. 2. Monte Carlo/S_N structure, A1/U235 problem.

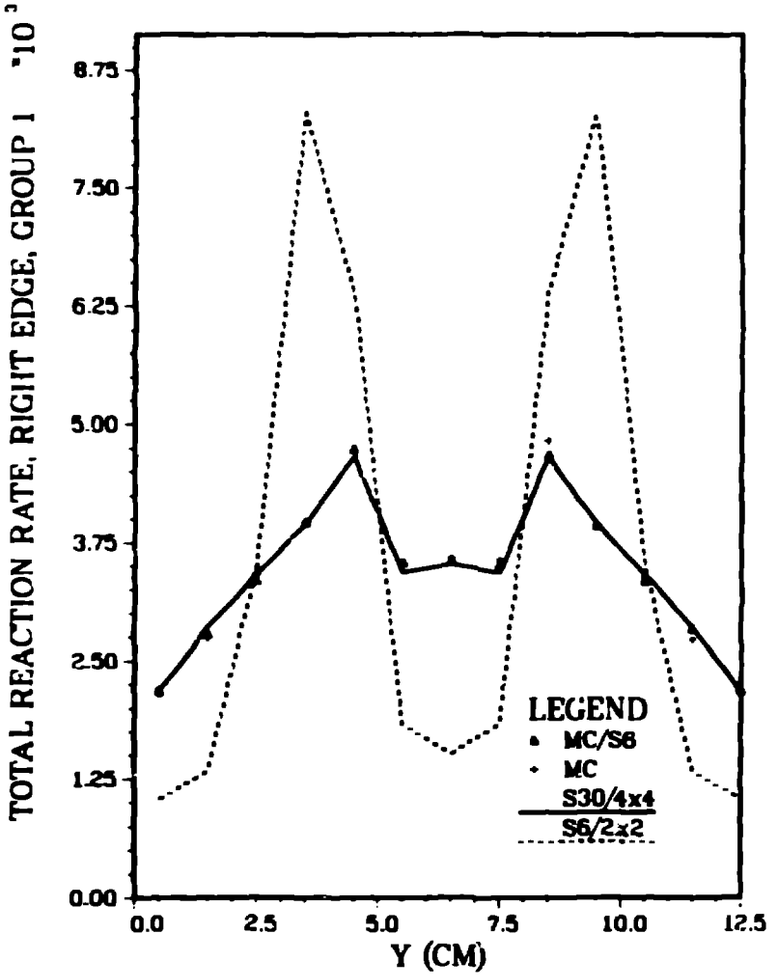

Fig. 3. Total reaction rates, x = 9.5 Cm, Group 1.

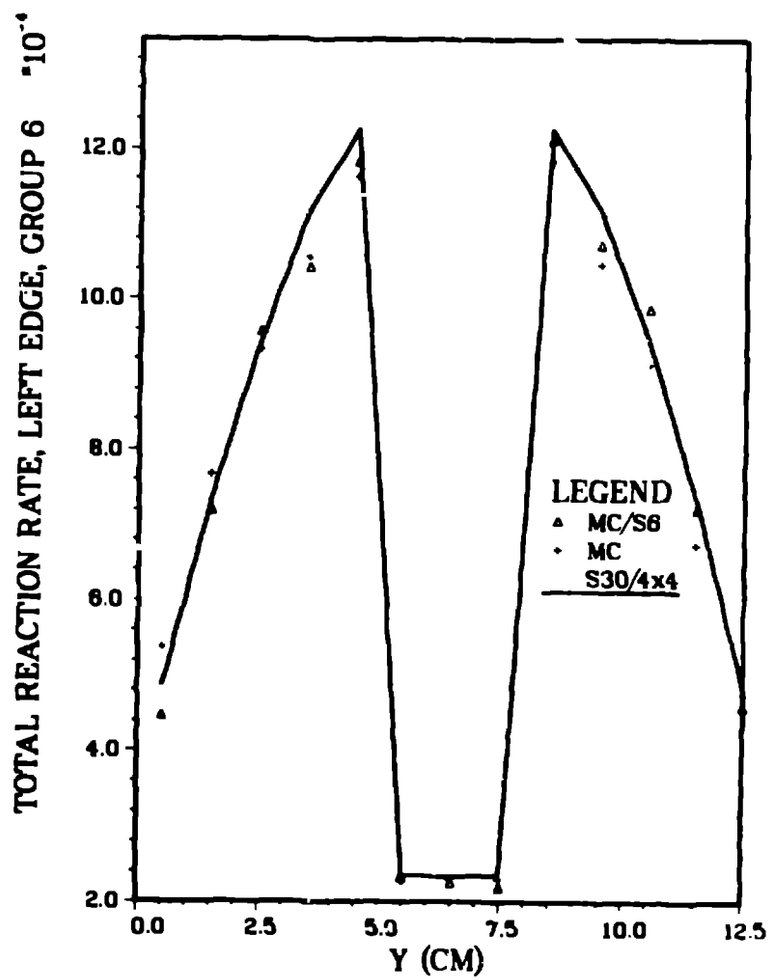

Fig. 4. Total reaction rates, x = .5 Cm, Group 6.

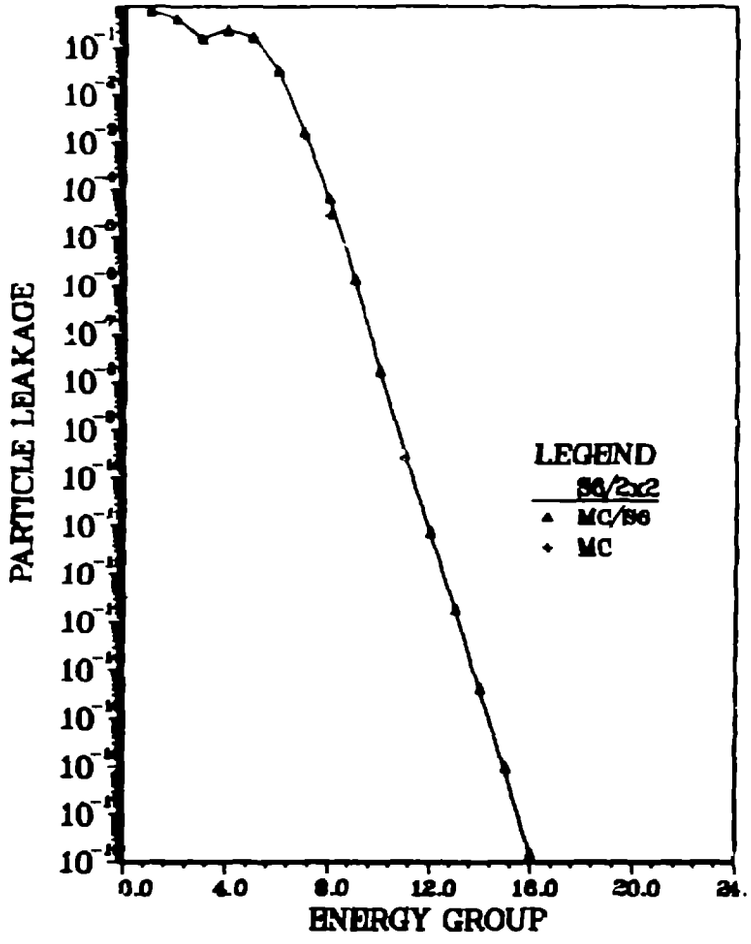

Fig. 5. Particle leakage, A1/U235 problem.

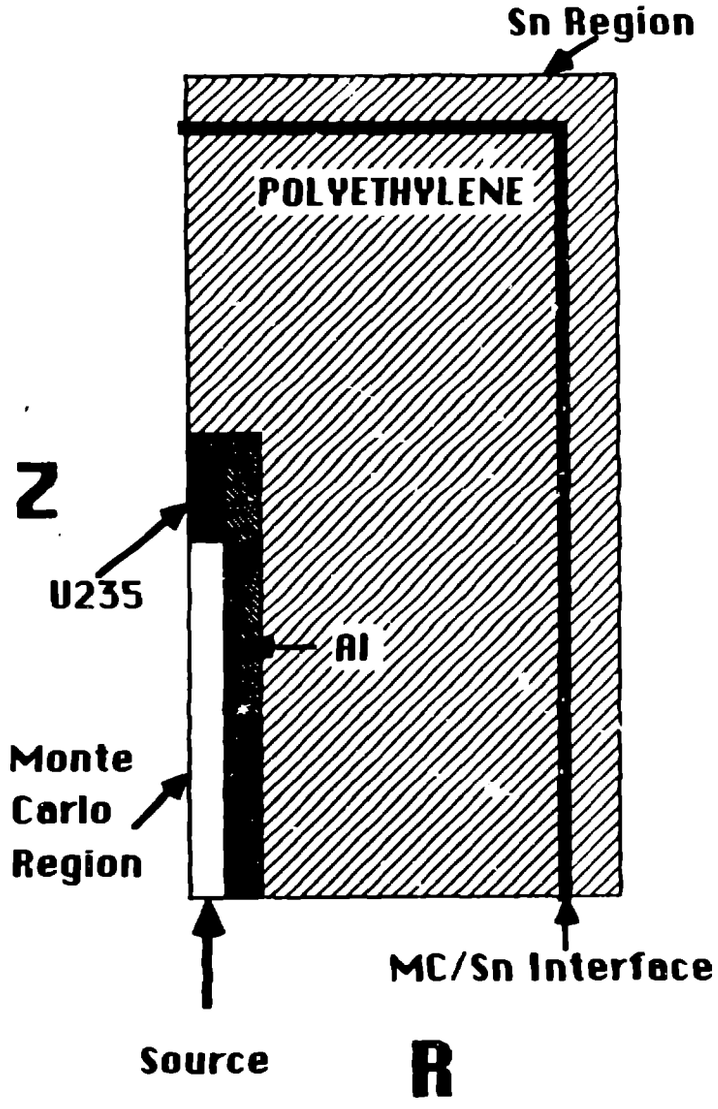

Fig. 6. Beam problem geometry.

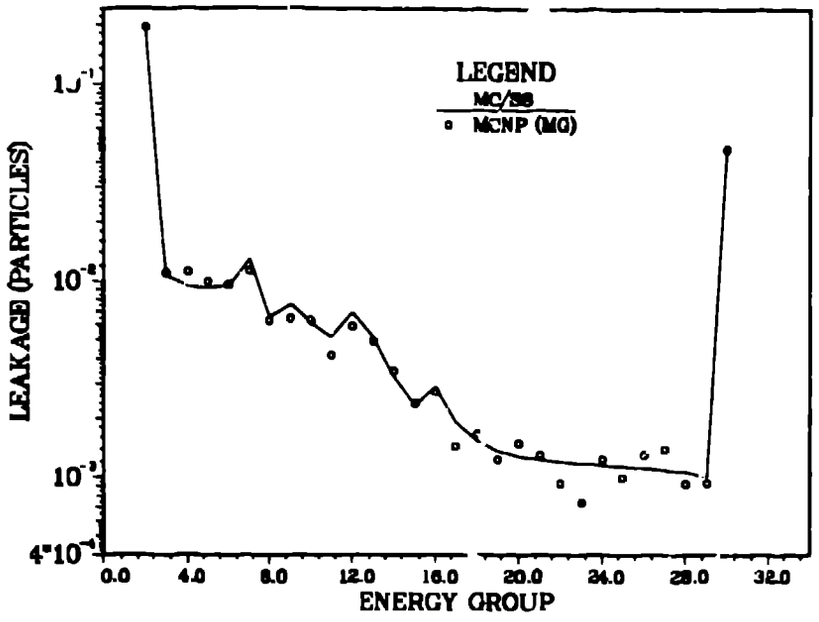

Fig. 7. Top leakage. beam problem.

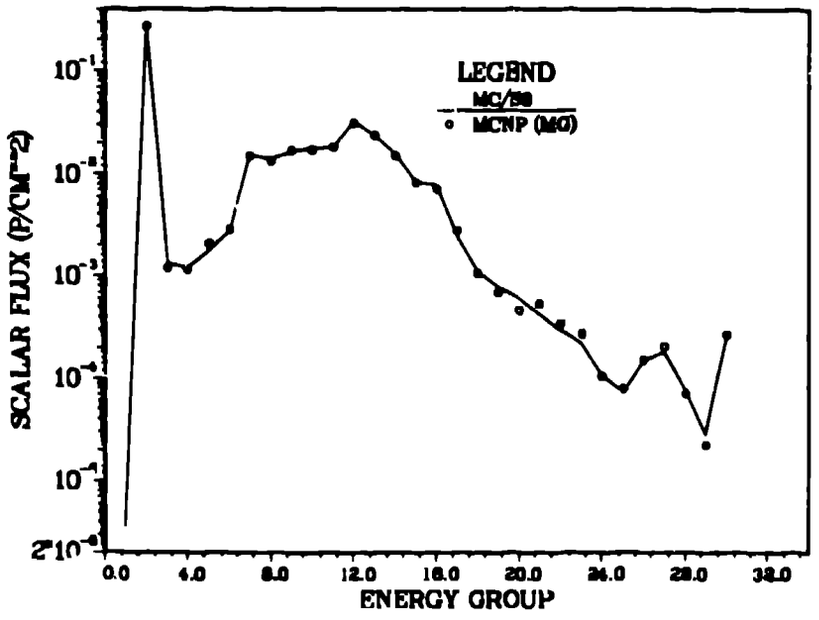

Fig. 8. Scalar flux in U235 target, beam problem.